

Transformation of Three-Connected Silicon Nets in CaSi_2

JÜRGEN EVERS

*Institut für Anorganische Chemie der Universität,
Meiserstrasse 1, D-800 München 2, Germany*

Received July 17, 1978

Up to 40 kbar and 1100°C, CaSi_2 is dimorphic. Trigonal/rhombohedral CaSi_2I (CaSi_2 -type structure) with corrugated layers of three-connected Si atoms can be transformed by a high pressure-high temperature treatment into tetragonal CaSi_2II (α - ThSi_2 -type structure) with a three-dimensional net of three-connected Si atoms. The silicon net of CaSi_2II is slightly distorted from the topologically simplest tetragonal three-dimensional three-connected net derived on a geometrical basis. In order to correlate crystal chemical with thermochemical data the transformation between both polymorphs of CaSi_2 has been studied at equilibrium and nonequilibrium conditions. The pressure-temperature phase diagram of CaSi_2 has been investigated by X-ray technique in quenched samples. From the slope of the equilibrium line and the change in molar volume the approximate values of the entropy and energy of transformation $\text{CaSi}_2(\text{I-II})$ have been determined $\Delta S = 3.2$ e.u., $\Delta U = 4.9$ kcal/mole. Under nonequilibrium conditions the transformation $\text{CaSi}_2(\text{II-I})$ yielded $\Delta H = -4.2$ kcal/mole at 500°C and ambient pressure in a DTA apparatus. Complete transformation of metastable CaSi_2II can be achieved within 5 min at a heating rate of 20°C/min. Due to the relatively high speed of transformation simple structural relations between both polymorphs of CaSi_2 are discussed.

Introduction

Corrugated layers of three-connected metalloid atoms in divalent metal disilicides and digermanides $M\text{Si}_2$ and $M\text{Ge}_2$ ($M = \text{Yb}, \text{Ca}, \text{Eu}, \text{Sr}, \text{Ba}$) are reported to be stacked in three different arrangements. In trigonal EuGe_2 (1), space group $D_{3d}^3-P\bar{3}m1$, the simplest stacking is found. In the [001] direction the structure is repeated after only one corrugated layer of three-connected Ge atoms. However, different stacking can be obtained from this structure if the layers are shifted to each other by $(a/3)3^{1/2}$ in the trigonal [110] direction and/or the layers are rotated by 180° around the layer normal. In the TR3 modification of trigonal/rhombohedral CaSi_2 (2, 3), space group $D_{3d}^5-R\bar{3}m$, corrugated layers of three-connected Si atoms are shifted without rotation and

achieve periodicity in the [001] direction after three layers. In addition to shifting of corrugated layers in the TR6 modification of trigonal/rhombohedral CaSi_2I (4), space group $D_{3d}^5-R\bar{3}m$, every second layer is here rotated by 180° around layer normal. In this case the structure is repeated after six layers in the [001] direction. Different stacking in both modifications of CaSi_2 seems to be effected by purity and stoichiometry.

By a high pressure-high temperature (HPHT) treatment (e.g., 40 kbar, 1000°C) trigonal/rhombohedral CaSi_2I (CaSi_2 -type structure) with corrugated layers of three-connected Si atoms can be transformed into tetragonal CaSi_2II (5–9) (α - ThSi_2 -type structure) (10) with a three-dimensional net of three-connected Si atoms. This net is slightly distorted from the topologically

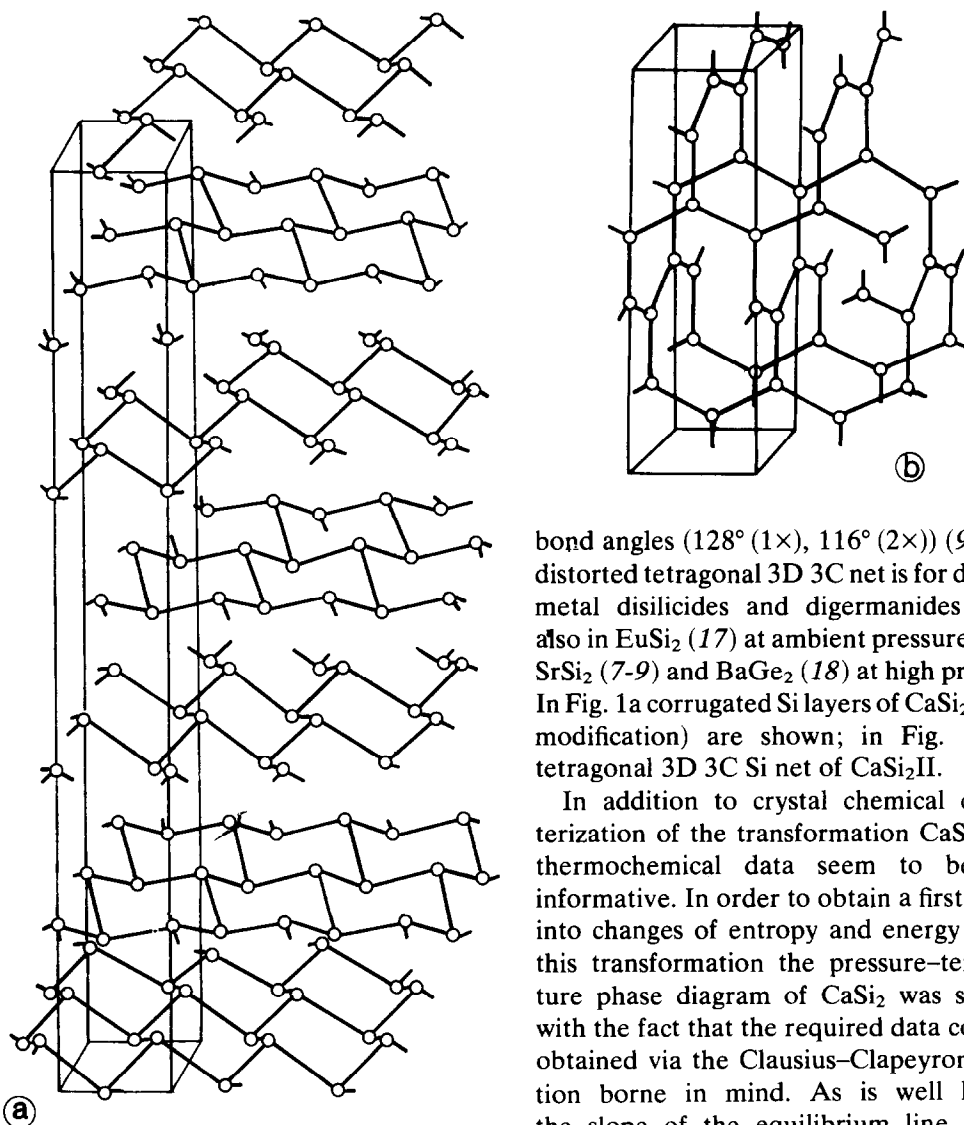


FIG. 1. (a) Corrugated layers of three-connected silicon atoms in trigonal/rhombohedral CaSi_2I (TR6 modification). (b) Three-dimensional three-connected silicon net in tetragonal CaSi_2II .

simplest tetragonal three-dimensional three-connected (3D 3C) net which has been derived on a geometrical basis by Wells (11–16). Instead of a coplanar group of four equidistant Si atoms with equal bond angles of 120° the repeat unit in the distorted 3D 3C net of CaSi_2II is coplanar, but not equidistant (2.34 \AA ($1\times$), 2.38 \AA ($2\times$)) and not with equal

bond angles (128° ($1\times$), 116° ($2\times$)) (9). This distorted tetragonal 3D 3C net is for divalent metal disilicides and digermanides found also in EuSi_2 (17) at ambient pressure and in SrSi_2 (7–9) and BaGe_2 (18) at high pressure. In Fig. 1a corrugated Si layers of CaSi_2I (TR6 modification) are shown; in Fig. 1b the tetragonal 3D 3C Si net of CaSi_2II .

In addition to crystal chemical characterization of the transformation $\text{CaSi}_2(\text{I-II})$ thermochemical data seem to be very informative. In order to obtain a first insight into changes of entropy and energy during this transformation the pressure–temperature phase diagram of CaSi_2 was studied, with the fact that the required data could be obtained via the Clausius–Clapeyron equation borne in mind. As is well known, the slope of the equilibrium line $\Delta P/\Delta T$ is related to changes in entropy and actual molar volume. From P–T equilibrium conditions in connection with entropy change the transformation energy can be calculated.

Tetragonal CaSi_2II is quenchable and can be stored at room temperature and pressure for long periods without showing any change. However, when this phase is heated to 450°C at ambient pressure complete retransformation into CaSi_2I is achieved. Therefore, the change in energy during this exothermic process can be easily measured in a cali-

brated DTA apparatus, although one obtains no equilibrium data of transformation. Nevertheless, transformation of metastable (at 500°C and ambient pressure) tetragonal SrSi_2II (α - ThSi_2 -type structure) into stable cubic SrSi_2I in a DTA apparatus yielded a 20% lower value of the transformation energy than that for equilibrium conditions obtained via the Clausius–Clapeyron equation (nonequilibrium $\text{SrSi}_2(\text{II-I})$ $\Delta H = -1.6 \pm 0.3$ kcal/mole; equilibrium $\text{SrSi}_2(\text{I-II})$ $\Delta U = 1.9 \pm 0.4$ kcal/mole) (19, 20). Therefore, the nonequilibrium value of the transformation $\text{CaSi}_2(\text{II-I})$ at ambient pressure can be considered as a rough test for the equilibrium value of the transformation $\text{CaSi}_2(\text{I-II})$. In addition, a first insight into the speed of transformation can be derived from the nonequilibrium experiment. This must be very informative for better understanding the transformation of corrugated layers of three-connected Si atoms into the tetragonal 3D 3C Si net in CaSi_2 .

Experimental

Sample preparation. High-purity CaSi_2I was prepared by inductive heating of high-ohmic silicon with ultrahigh-vacuum-distilled calcium (21) in a high-vacuum tight cold copper boat. Additional details have been given elsewhere (9, 19).

High-pressure–high-temperature treatment. High pressure up to 40 kbar was generated in a belt-type apparatus (22). Calibration of pressure was performed measuring the discontinuities of resistance at ambient temperature in the transformations of $\text{Ce}(\text{I-II})$, $\text{Bi}(\text{I-II})$, and $\text{Tl}(\text{I-III})$ with alternating current. Calibration of temperature was obtained via wattages against chromel–alumel thermocouples. More details of pressure and temperature calibration are quoted elsewhere (20). In the P–T diagram pressure is believed to be correct within ± 2 kbar and temperatures (via wattages) within $\pm 25^\circ\text{C}$. For the phase diagram studies defined P–T conditions were maintained for 15 min.

After quenching to room temperature pressure was released.

X-Ray characterization. Phase analyses in quenched samples were performed by the Debye–Scherrer technique in a Straumanis arrangement (Ni-filtered copper K_α , 114.6 mm Seifert camera).

Differential thermal analysis. Nonequilibrium transformation $\text{CaSi}_2(\text{II-I})$ at ambient pressure was investigated in a high-vacuum tight Linseis-DTA apparatus under dynamic flow of argon ($20\text{ cm}^3/\text{min}$) at a heating rate of $20^\circ\text{C}/\text{min}$ in tantalum crucibles with Pt90Rh10–Pt thermocouples. Typical weights of CaSi_2II for DTA runs were in the range 27–30 mg. Additional details and calibration have been quoted elsewhere (19).

Results

In Table I the structural data for trigonal/rhombohedral CaSi_2I (TR6 modification) (2–4) and tetragonal CaSi_2II (9) are presented.

In Fig. 2 the pressure-temperature phase diagram of CaSi_2 up to 40 kbar and 1100°C derived from 17 different P–T experiments is shown. No attempt was made to resolve curvature of the phase boundary. In a quasiunary approach the slope of the equilibrium line is $\Delta P/\Delta T = -60$ bar/deg. For example, at approximately 32 kbar and 1000°K CaSi_2I and CaSi_2II coexist.

The equilibrium entropy change $\text{CaSi}_2(\text{I-II})$ is obtained if $\Delta P/\Delta T$ is multiplied by the actual change in molar volume ΔV_T^P under HPHT conditions (e.g., 32 kbar, 1000°K). However, ΔV_T^P can be obtained from the change in molar volume at ambient conditions ΔV_{298} ($= -2.19 \approx -2.2\text{ cm}^3/\text{mole}$; Table I) if the coefficients of isobaric thermal expansion α and isothermal compressibility χ are known. Since α and χ are proportional to each other (Grüneisen parameter) (23) the influence of χ values on ΔV_T^P can be

TABLE I
STRUCTURAL DATA FOR TRIGONAL/RHOMBOHEDRAL AND FOR TETRAGONAL CaSi_2

Phase	Normal pressure ^a	High pressure
Crystal class	Trigonal/rhombohedral	Tetragonal
Space group	$D_{3d}^5-R\bar{3}m$	$D_{4h}^{19}-I4_1/amd$
Lattice parameters (Å)	$a = 3.855 \pm 0.005$ $c = 30.6 \pm 0.1$	$a = 4.283 \pm 0.003$ $c = 13.52 \pm 0.01$
Cell volume (Å ³)	393.8	248.0
Density (g/cm ³)		
Observed	2.46	2.5 ₅
X-Ray	2.44	2.578
Molar volume (cm ³ /mole)	39.53	37.34
Formula units	6	4
Positions	6 Ca in 6c (0, 0, z)(0, 0, \bar{z}) $(\frac{1}{3}, \frac{2}{3}, \frac{2}{3} + z)(\frac{1}{3}, \frac{2}{3}, \frac{2}{3} - z)$ $(\frac{2}{3}, \frac{1}{3}, \frac{1}{3} + z)(\frac{2}{3}, \frac{1}{3}, \frac{1}{3} - z)$ $z = 0.083$	4 Ca in 4a (0, 0, 0)(0, $\frac{1}{2}$, $\frac{1}{4}$) $(\frac{1}{2}, \frac{1}{2}, \frac{1}{2})(\frac{1}{2}, 0, \frac{3}{4})$
	6 Si _I in 6c $z = 0.183$	8 Si in 8e (0, 0, z)(0, 0, \bar{z}) $(0, \frac{1}{2}, \frac{1}{4} + z)(0, \frac{1}{2}, \frac{1}{4} - z)$ $(\frac{1}{2}, \frac{1}{2}, \frac{1}{2} + z)(\frac{1}{2}, \frac{1}{2}, \frac{1}{2} - z)$ $(\frac{1}{2}, 0, \frac{3}{4} + z)(\frac{1}{2}, 0, \frac{3}{4} - z)$ $z = 0.413_5$
	6 Si _{II} in 6c $z = 0.350$	

^a TR6 modification

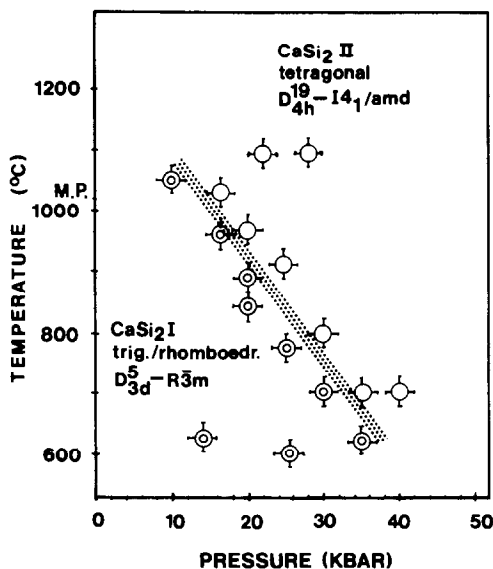


FIG. 2. Pressure-temperature phase diagram of CaSi_2 .

estimated if α values are known. Measurement of thermal expansion of CaSi_2 I and II at ambient pressure showed only a small difference. Therefore, differences between χ values must also be small so that ΔV_T^P can be identified with ΔV_{298} (to a good approximation). With $\Delta V_{298} = -2.2 \text{ cm}^3/\text{mole}$ one calculates the entropy change $\text{CaSi}_2(\text{I-II})$, $\Delta S = 3.2 \pm 0.6 \text{ e.u.}$ and the energy change $\Delta U = 4.9 \pm 1.0 \text{ kcal/mole}$.

Table II shows the thermochemical data derived from two different DTA runs under nonequilibrium conditions. A typical first heating run is presented in Fig. 3a and a second one after transformation in Fig. 3b. The significant feature of these figures is that the transformation $\text{CaSi}_2(\text{II-I})$ at 500°C and ambient pressure is exothermic and irreversible. The average value of the energy of this transformation $\Delta H = -4.2 \pm 0.8 \text{ kcal/mole}$ has been determined. Complete trans-

TABLE II
THERMOCHEMICAL DATA OF THE PHASE TRANSFORMATION TETRAGONAL INTO TRIGONAL/RHOMBOHEDRAL CaSi_2 AT AMBIENT PRESSURE

Transformation character	Exothermic irreversible	
	20°C/min	
Heating rate		
Sample weight (mg)	27.95	30.07
Transformation peak (°C)		
Start	482	478
Medium	533	528
End	578	573
Energy of transformation at ambient pressure (cal/mole)	-4165 ± 833	-4286 ± 857
Average value of the transformation energy at ambient pressure (kcal/mole)	-4.2 ± 0.8	

formation $\text{CaSi}_2(\text{II-I})$ at ambient pressure is achieved within 5 min at a heating rate of 20°C/min (Fig. 3a, Table 1).

Discussion

By inspection of Table III it is clear that coordination numbers are increased by HPHT treatment of CaSi_2I , in agreement with general experience. Trigonal/rhombohedral CaSi_2I (TR6 modification) shows 7:3.5 coordination (Ca has seven Si neighbors; Si_I has four Ca and Si_II three Ca neighbors), whereas 12:6 coordination is found for tetragonal CaSi_2II . Interestingly, three-connection of silicon atoms is retained in

tetragonal CaSi_2II . Both phases of CaSi_2 and also all investigated polymorphs of divalent metal disilicides and digermanides at ambient and at high pressure satisfy the generalized $8-N$ rule derived for polyanionic compounds (24-26).

The transformation of the tetragonal 3D 3C Si-net of CaSi_2II into corrugated Si-layers is relatively rapid. Under nonequilibrium conditions complete transformation $\text{CaSi}_2(\text{II-I})$ is achieved within 5 min (Table II, Fig. 3). Under comparable experimental conditions the nonequilibrium transformation speed for $\text{SrSi}_2(\text{II-I})$ (19) is the same. Nevertheless, from these observations no quantitative conclusions can be drawn

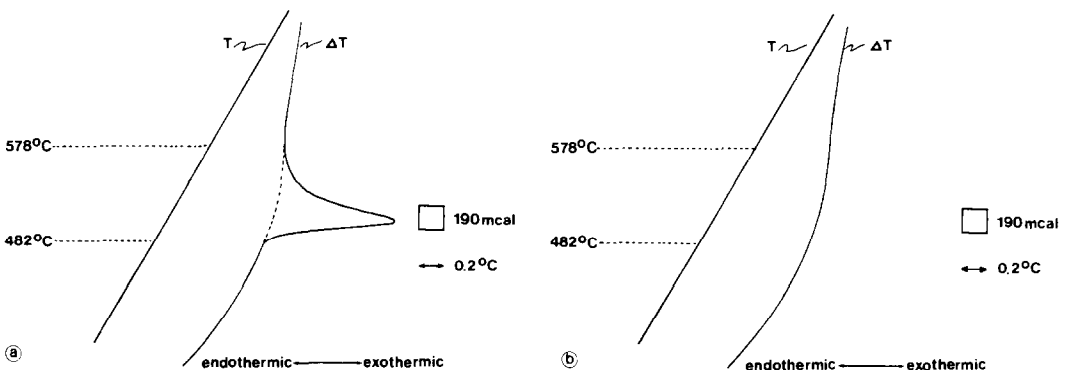


FIG. 3. (a) Thermogram of first heating cycle of 27.95 mg tetragonal CaSi_2II at ambient pressure. (b) Thermogram of second heating cycle.

TABLE III
NUMBER OF NEIGHBORS AND BOND DISTANCES
FOR TRIGONAL/RHOMBOHEDRAL AND
TETRAGONAL CaSi_2

Phase	Trigonal/ rhombohedral ^a (Å)	Tetragonal (Å)
Calcium neighbors	6 Ca 3.86	4 Ca 4.00
	6 Si 3.03	4 Si 3.08
	1 Si 3.06	8 Si 3.25
Silicon neighbors	3 Si 2.45	1 Si 2.3 ₄
		2 Si 2.3 ₈
	3 Ca 3.03	2 Ca 3.08
	(1 Ca 3.06) ^b	4 Ca 3.25

^a TR6 modification after Böhm and Hassel (4) (1927).

^b There are two different Si atoms; Si_I with 3 Ca 3.03 Å and 1 Ca 3.06 Å and Si_{II} with 3 Ca 3.03 Å.

since equilibrium conditions are missing. It is also known that crystal order and impurities influence transformation kinetics. However, the transformation of at ambient pressure quenchable α -ThSi₂ (high-temperature phase) with a nearly ideal tetragonal 3D 3C Si net into stable β -ThSi₂ (low-temperature phase) with planar Si layers is not as rapid as in CaSi₂(II-I) or in SrSi₂(II-I) (27).

If one looks for crystal chemical relations between CaSi₂I and II it must be considered that total breakdown of the old lattice in order to build up the new one is avoided. Otherwise such a total reconstructive transformation (29, 30) will proceed sluggishly. A projection of two unit cells (lying above) of the Si net I down the orthohexagonal *b* axis ($= a_{\text{trig}} \cdot 3^{1/2}$) is shown in Fig. 4a. Since one orthohexagonal cell of CaSi₂I contains twice the number of formula units than the trigonal one, 48 ($= 2 \cdot 2 \cdot 12$) silicon atoms are found here in corrugated layers. The silicon atoms in three pairs of the six layers are at different heights $n \cdot a_{\text{trig}} \cdot 3^{1/2}$. Due to the geometry of equilateral triangles accepted values for *n* are $\frac{1}{6}$, $\frac{2}{6}$, $\frac{4}{6}$, and $\frac{5}{6}$. Corrugated (cyclohexane chair-like) Si hexagons in one layer can be

considered as built up by flat distorted "helices" which repeat after four atoms (Fig. 5a). Besides the different "diameters" (1.93 and 1.01 Å, Fig. 5a) the "helices" are not true 4₃- or 4₁-helices since there is no constant sense in screw motion (Fig. 5a). This is a consequence of corrugating the layers. In two orthohexagonal unit cells of the TR6 modification of CaSi₂I there exist six different distorted flat "helices."

In Fig. 4b a projection of six unit cells of the tetragonal 3D 3C Si net II down the *c*_{tetr} axis is shown. These six unit cells also contain 48 ($= 6 \cdot 8$) silicon atoms. The tetragonal 3D 3C net can be built up by true 4₁-helices (Fig. 5b). Further details are discussed in (19).

Comparing Figs. 4a, b and 5a, b one sees the striking difference between the two Si nets. For two of the three axes of the cells considered with equal number of silicon atoms, good agreement is found: $a_{\text{trig}} = 3.86 \text{ Å} \approx a_{\text{tetr}} = 4.28 \text{ Å}$ and $2 \cdot 3^{1/2} a_{\text{trig}} = 13.37 \text{ Å} \approx c_{\text{tetr}} = 13.52 \text{ Å}$. However, the third relation, $\frac{1}{6} \cdot c_{\text{trig}} = 5.10 \text{ Å} \approx a_{\text{tetr}} = 4.28 \text{ Å}$, shows the greatest difference. For transformation CaSi₂(I-II) one-third of bonds between the three-connected Si atoms in the corrugated layers have to be broken, and the "diameter" of the distorted helices must increase in one direction (Figs. 5a, b) (1.01 Å \rightarrow 2.14 Å). After additional minor changes in "helix" dimensions (1.93 Å \rightarrow 2.14 Å and 13.37 Å \rightarrow 13.52 Å), Si atoms have to rearrange in the helices and reconstruct the third Si-Si bond within the tetragonal 3D 3C net. Therefore this transformation must be considered as a reconstructive one (28, 29), as also observed for SrSi₂ (19).

Although both nonequilibrium transformations CaSi₂(II-I) and SrSi₂(II-I) can be performed within the same time, crystal chemical differences between CaSi₂I and CaSi₂II are greater than those between SrSi₂I and SrSi₂II. These differences are reflected in the thermochemical data of both

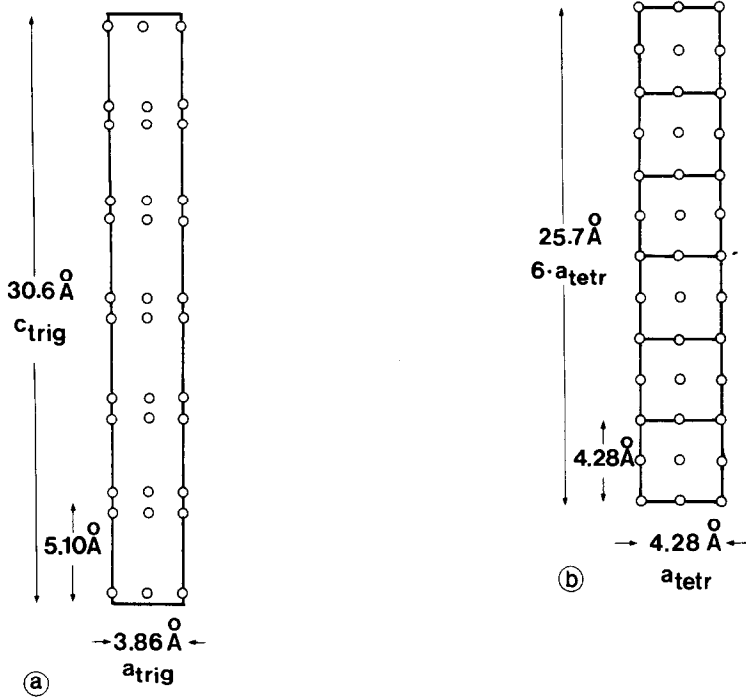


FIG. 4. (a) Projection of two unit cells with corrugated layers of CaSi_2I (TR6 modification) down orthohexagonal b axis. (b) Projection of six unit cells of tetragonal 3D 3C Si net down tetragonal c axis.

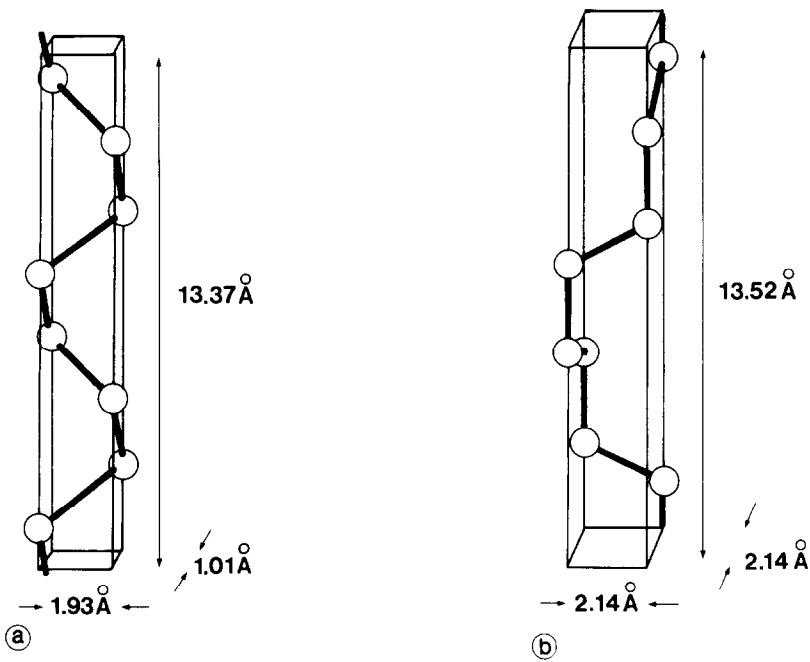


FIG. 5. (a) Flat distorted "helices" which repeat after four atoms in Si net of CaSi_2I (TR6 modification). (b) 4_1 -Helix of the tetragonal 3D 3C Si Net of CaSi_2II .

transformations. Since the slope of the equilibrium line of $\text{CaSi}_2(\text{I-II})$ $\Delta P/\Delta T = -60$ bar/deg and also the change in molar volume is greater, $\Delta V = -2.2$ cm³/mole ($\text{SrSi}_2(\text{I-II})$: $\Delta P/\Delta T = -47$ bar/deg, $\Delta V = -1.0$ cm³/mole), one calculates both a higher entropy change $\Delta S = 3.2 \pm 0.6$ e.u. and energy change $\Delta U = 4.9 \pm 1.0$ kcal/mole ($\text{SrSi}_2(\text{I-II})$: $\Delta S = 1.1 \pm 0.2$ e.u., $\Delta U = 1.9 \pm 0.4$ kcal/mole) (19, 20). Higher energy change is also found in the thermograms of the DTA runs for which one finds nonequilibrium $\text{CaSi}_2(\text{II-I})$ $\Delta H = -4.2 \pm 0.8$ kcal/mole, with a well-pronounced peak instead of a flat one for nonequilibrium $\text{SrSi}_2(\text{II-I})$ (19).

Tetragonal CaSi_2II is not high-temperature phase at ambient pressure. At the melting point of CaSi_2I ($1020^\circ\text{C} = 1293^\circ\text{K}$) one calculates approximately 0.8 kcal/mole (=16% of the total change) to be missing. Since CaSi_2II is the more densely packed phase ($\Delta V = -2.2$ cm³/mole) small pressures are sufficient near the melting point of CaSi_2I to generate the missing stabilization energy.

The different features between the structure types of CaSi_2I and II (CaSi_2 and $\alpha\text{-ThSi}_2$ types of structure, respectively) are shown if one lists the number of binary examples of the structure types found for divalent metal disilicides and digermanides at ambient and at HPHT conditions (Table IV). Ytterbium compounds have not been considered, due to the unsolved problem of stoichiometry. The greatest dependence of a structure type on the metallic radius is found for the CaSi_2 type because here only two compounds with the same metal (Ca) exist. On the other hand, present knowledge of the $\alpha\text{-ThSi}_2$ type with a tetragonal 3D 3C net indicates that it is the most variable one since it is found in $M\text{Si}_2$ or $M\text{Ge}_2$ compounds with four different divalent metals M ($M = \text{Ca}, \text{Eu}, \text{Sr}, \text{Ba}$). Also sensitive to changes of metallic radius is the SrSi_2 type with a cubic

TABLE IV
BINARY EXAMPLES OF STRUCTURE TYPES
KNOWN FOR DIVALENT METAL DISILICIDES AND
DIGERMANIDES^a

CaSi_2	CaSi_2I (2-4), CaGe_2I (30)
SrSi_2	SrSi_2I (31, 3, 32), BaSi_2III (33)
EuGe_2	EuGe_2I (1), SrGe_2II (34), BaSi_2II (7, 8, 35)
BaSi_2	SrGe_2I (37), BaSi_2I (36, 3), BaGe_2I (37)
$\alpha\text{-ThSi}_2$	CaSi_2II (5-9), EuSi_2I (17), SrSi_2II (7-9, 19, 20), BaGe_2II (18)

^a Due to the unsolved problem of stoichiometry Yb compounds are not considered here..

3D 3C net known for SrSi_2I and BaSi_2III (33). From the dependence of lattice parameters on the metallic radius in solid solutions $M_{1-x}M_x\text{Si}_2$ ($M, M' = \text{Ca}, \text{Eu}, \text{Sr}, \text{Ba}$) with SrSi_2 -type lattice parameters for hypothetical EuSi_2 and CaSi_2 with this structure type have been extrapolated (38). From these data it seems that the structure types observed up to now at ambient pressure are more densely packed than those with a cubic 3D 3C net (SrSi_2 type). The cavities in this net seem too large for europium and calcium to stabilize this structure type. From geometrical relations between the ideal cubic and tetragonal 3D 3C nets it has been calculated that for a constant Si-Si bond distance of 2.39 Å the unit-cell volume of the cubic 3D 3C net is much larger (308.9 \AA^3) than that of the tetragonal one (245.8 \AA^3) (19). This is in agreement with the experimental fact that for strontium ($r_{\text{Sr}} = 2.151 \text{ \AA}$ CN 12) and thorium ($r_{\text{Th}} = 1.798 \text{ \AA}$) nearly the same Si-Si bond distance of 2.39 Å is achieved in the cubic and tetragonal 3D 3C nets, respectively ($V_{\text{SrSi}_2\text{I}} = 279.1 \text{ \AA}^3$, $V_{\text{ThSi}_2\text{II}} = 245.8 \text{ \AA}^3$ for four formula units each).

Also in agreement with the interpretation that for CaSi_2 with SrSi_2 -type structure the metallic radius of Ca ($r_{\text{Ca}} = 1.974 \text{ \AA}$) seems

to be too small is that for large barium ($r_{\text{Ba}} = 2.243 \text{ \AA}$) transformation of corrugated layers in BaSi_2II with EuGe_2 -type structure into the cubic 3D 3C net was successful (33). Investigation of the pressure-temperature phase diagram of trimorphic BaSi_2 is still in progress (39).

Acknowledgment

Financial support of this work by Deutsche Forschungsgemeinschaft under Contract Ev 14/2 is gratefully announced.

References

1. E. I. GLADYSHEVSKII, *Dopov. Akad. Nauk Ukr. RSR* **2**, 209 (1964).
2. K. H. JANZON, H. SCHÄFER, AND A. WEISS, *Z. Naturforsch.* **23b**, 1544 (1968).
3. K. H. JANZON, H. SCHÄFER, AND A. WEISS, *Z. Anorg. Allg. Chem.* **372**, 87 (1970).
4. J. BÖHM AND O. HASSEL, *Z. Anorg. Allg. Chem.* **160**, 152 (1927).
5. M. S. SILVERMAN AND J. R. SOULEN, *J. Phys. Chem.* **67**, 1919 (1963).
6. D. B. MCWHAN, V. B. COMPTON, M. S. SILVERMAN, AND J. R. SOULEN, *J. Less-Common Metals* **12**, 75 (1967).
7. J. EVERS AND A. WEISS, GDCh-Festcolloquium in honour of the 80th birthday of Prof. W. Klemm, Münster, February 1976.
8. J. EVERS, G. OEHLINGER, AND A. WEISS, Third European Crystallogr. Meeting, Zürich, September 1976.
9. J. EVERS, G. OEHLINGER, AND A. WEISS, *J. Solid State Chem.* **20**, 173 (1977).
10. G. BRAUER AND A. MITIUS, *Z. Anorg. Allg. Chem.* **249**, 325 (1942).
11. A. F. WELLS, *Acta Crystallogr.* **7**, 535 (1954).
12. A. F. WELLS, *Acta Crystallogr.* **9**, 23 (1956).
13. A. F. WELLS AND R. R. SHARPE, *Acta Crystallogr.* **16**, 857 (1963).
14. A. F. WELLS, *Acta Crystallogr.* **B28**, 711 (1972).
15. A. F. WELLS, "Structural Inorganic Chemistry", Oxford Univ. Press (Clarendon), London, 1975.
16. A. F. WELLS, "Three-Dimensional Nets and Polyhedra", Wiley, New York/London/Sydney/Toronto, 1977.
17. J. A. PERRI, I. BINDER, AND B. POST, *J. Phys. Chem.* **63**, 616 (1959).
18. J. EVERS, G. OEHLINGER, AND A. WEISS, *Z. Naturforsch.* **32b**, 1352 (1977).
19. J. EVERS, *J. Solid State Chem.* **24**, 199 (1978).
20. J. EVERS, submitted to *J. Phys. Chem. Solids*.
21. J. EVERS, E. KALDIS, J. MUHEIM, AND A. WEISS, *J. Less-Common Metals* **30**, 83 (1973).
22. K.-J. RANGE AND R. LEEB, *Z. Naturforsch.* **30b**, 889 (1975).
23. G. BUSCH AND H. SCHADE, "Vorlesungen über Festkörperphysik," Birkhäuser Verlag, Basel/Stuttgart, 1973, p. 114.
24. E. MOOSER AND W. B. PEARSON, *J. Electr.* **1**, 1 (1956).
25. F. HULLIGER AND E. MOOSER, *J. Phys. Chem. Solids* **24**, 283 (1963).
26. F. HULLIGER AND E. MOOSER, *Progr. Solid State Chem.* (1965) 330.
27. J. EVERS, to be published.
28. M. J. BUERGER, "Phase Transformations in Solids," (R. SMOLUCHOWSKI, Ed.), p. 183, Wiley, New York, 1951.
29. M. J. BUERGER, *Fortschr. Mineral.* **39**, 9 (1961).
30. H. J. WALLBAUM, *Naturwissenschaften* **32**, 76 (1944).
31. K. H. JANZON, H. SCHÄFER, AND A. WEISS, *Angew. Chem.* **77**, 258 (1965). *Angew. Chem. Int. Ed. Engl.* **4**, 245 (1965).
32. G. E. PRINGLE, *Acta Crystallogr.* **B28**, 2326 (1972).
33. J. EVERS, G. OEHLINGER, AND A. WEISS, *Angew. Chem.* **90**, 562 (1978). *Angew. Chem. Int. Ed. Engl.* **17**, 538 (1978).
34. J. EVERS, G. OEHLINGER, AND A. WEISS, to appear in *Z. Naturforsch.*
35. J. EVERS, G. OEHLINGER, AND A. WEISS, *Angew. Chem.* **89**, 673 (1977). *Angew. Chem. Int. Ed. Engl.* **16**, 659 (1977).
36. K. H. JANZON, H. SCHÄFER, AND A. WEISS, *Angew. Chem.* **75**, 451 (1963). *Angew. Chem. Int. Ed. Engl.* **2**, 393 (1963).
37. K. H. JANZON, H. SCHÄFER, AND A. WEISS, *Z. Naturforsch. B* **23**, 878 (1968).
38. J. EVERS, G. OEHLINGER, AND A. WEISS, to appear in *J. Less-Common Metals*.
39. J. EVERS, to be published.